

OpenVTON-Bench: A Large-Scale High-Resolution Benchmark for Controllable Virtual Try-On Evaluation

Jin Li^{*1,2} Tao Chen^{*1} Shuai Jiang¹ Weijie Wang¹ Jingwen Luo¹ Chenhui Wu^{1†}

Abstract

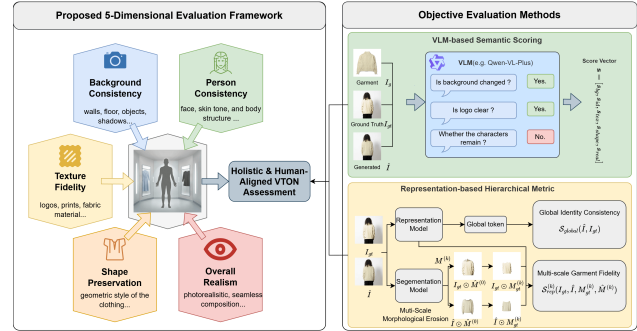
Recent advances in diffusion models have significantly elevated the visual fidelity of Virtual Try-On (VTON) systems, yet reliable evaluation remains a persistent bottleneck. Traditional metrics struggle to quantify fine-grained texture details and semantic consistency, while existing datasets fail to meet commercial standards in scale and diversity. We present OpenVTON-Bench, a large-scale benchmark comprising approximately 100K high-resolution image pairs (up to 1536×1536). The dataset is constructed using DINOv3-based hierarchical clustering for semantically balanced sampling and Gemini-powered dense captioning, ensuring a uniform distribution across 20 fine-grained garment categories. To support reliable evaluation, we propose a multi-modal protocol that measures VTON quality along five interpretable dimensions: background consistency, identity fidelity, texture fidelity, shape plausibility, and overall realism. The protocol integrates VLM-based semantic reasoning with a novel Multi-Scale Representation Metric based on SAM3 segmentation and morphological erosion, enabling the separation of boundary alignment errors from internal texture artifacts. Experimental results show strong agreement with human judgments (Kendall’s τ of 0.833 vs. 0.611 for SSIM), establishing a robust benchmark for VTON evaluation.

1. Introduction

Image-based Virtual Try-On (VTON) is predicated upon synthesizing a photorealistic image of a target person wearing a selected garment, while meticulously preserving their identity, pose, and the garment’s visual attributes (Yang et al., 2025; Wang et al., 2025; Choi et al., 2021b). As

^{*}Equal contribution [†]Project lead and corresponding author. ¹Renxing Intelligence, Hangzhou, China ²Hangzhou Dianzi University, Hangzhou, China. Correspondence to: Chenhui Wu <wuchenhui@renxing.co>.

Preprint. February 2, 2026.



a cornerstone technology for e-commerce and the digital fashion industry, VTON systems are increasingly expected to deliver high-fidelity results under diverse and commercially relevant conditions. The advent of latent diffusion models has catalyzed a paradigm shift, dramatically enhancing the quality and resolution of VTON outputs (Kim et al., 2024; Yang et al., 2024; Kim et al., 2025; Shim et al., 2024). Consequently, the research focus is rapidly pivoting from the foundational challenge of *how to generate* to the more critical and nuanced question of *how to robustly evaluate*. As generative models iterate at an unprecedented pace, this widening gap between generation and evaluation becomes increasingly perilous, potentially misleading the field toward optimizing for models that fail in real-world applications.

Despite the rapid evolution of diffusion-based try-on models, the evaluation infrastructure has failed to keep pace, creating a significant *misalignment* between generative capabilities and benchmarking standards. Prevailing benchmarks largely rely on legacy datasets such as VITON-HD (Choi et al., 2021b) and DressCode (Morelli et al., 2022). While foundational, these datasets suffer from a “**studio-centric bias**”—characterized by clean backgrounds, standardized poses, and restricted resolutions (typically capped at 1024×768). Such constrained environments fall short of stress-testing modern models, which must handle com-

Table 1. Comparison of Virtual Try-On Datasets. We compare OpenVTON-Bench with representative datasets in terms of scale, resolution, and accessibility. Unlike prior benchmarks that are either low-resolution or closed-source, our benchmark offers the largest open-source collection of high-fidelity images with $\min(H, W) \geq 1024$. *Open-Source*: ✓ denotes publicly available, × denotes closed.

Dataset	Year	Quantity	Resolution	Open-Source
VITON (Han et al., 2018)	2018	16,253	256 × 192	✓
VITON-HD (Choi et al., 2021b)	2021	13,679	1024 × 768	✓
DressCode (Morelli et al., 2022)	2022	53,792	1024 × 768	✓
SHHQ (Fu et al., 2022)	2022	231,176	1024 × 768	✓
StreetTryOn (Cui et al., 2024)	2024	14,453	512 × 320	✓
LH-400K (Li et al., 2024b)	2024	409,270	512 × 512	✓
VTBench (Xiaobin et al., 2025)	2025	2,933	-	×
VTONQA (Wei et al., 2026)	2026	8,132	256 ² ~ 4096 ²	×
OpenVTON-Bench (Ours)	2026	99,925	1024² ~ 1536²	✓

plex lighting, severe occlusions, and diverse body shapes in real-world commercial scenarios. Although recent initiatives like VTONQA (Wei et al., 2026) have attempted to introduce higher-resolution samples, they are often limited by small scales or restrictive licenses (non-open-source). This widens the chasm between the ever-improving visual fidelity of generated images and the capacity of existing benchmarks to reliably measure it. To bridge this gap, we introduce **OpenVTON-Bench**, a large-scale, high-resolution, and fully open-source benchmark designed to push the boundaries of realistic virtual try-on assessment.

This gap is further exacerbated by a reliance on conventional evaluation metrics that have become decoupled from human perceptual reality. Standard measures such as Fréchet Inception Distance (FID) (Heusel et al., 2017), Structural Similarity Index (SSIM) (Detlefsen et al., 2022), and Learned Perceptual Image Patch Similarity (LPIPS) (Zhang et al., 2018) operate primarily on global feature distributions or low-level patch similarities. While effective for assessing general image synthesis quality, these metrics suffer from “**semantic blindness**” in conditional tasks like VTON. They are notoriously insensitive to the localized yet critical failures: a generated image might achieve a favorable FID score by strictly adhering to the training set’s pixel statistics, yet fail catastrophically in preserving the garment’s brand identity (e.g., a distorted logo) or the user’s physical attributes (e.g., inconsistent body shape). Such artifacts—while statistically subtle to an Inception network—are immediately disqualifying in real-world commercial applications.

To surmount these limitations, we leverage the emerging “**LLM-as-a-Judge**” paradigm from Natural Language Processing (Zheng et al., 2023), where models serve as reliable surrogates for human evaluation. Adapting this philosophy to the visual domain, we propose a **VLM-as-a-Judge** framework for VTON assessment. In stark contrast to traditional metrics that reduce perceptual quality to opaque scalars, state-of-the-art Vision-Language Models (VLMs) (Bai et al., 2025; Zhu et al., 2025) enable *multimodal chain-of-thought*

reasoning. This capability allows them to scrutinize generated images against fine-grained instructions, identifying semantic misalignments that statistical metrics systematically overlook.

However, relying exclusively on semantic reasoning is inadequate, as VLMs often exhibit spatial imprecision and struggle to quantify subtle structural deformations in textile patterns (Xiaobin et al., 2025). We argue that robust evaluation demands a synergy between high-level semantic understanding and low-level structural verification. To this end, we introduce a **Multi-Modal Evaluation Protocol** that complements VLM-based semantic scrutiny with a **multi-scale representation-based garment fidelity metric**. While the VLM acts as a judge of holistic realism and identity consistency, our representation metric is tailored for fine-grained texture analysis: by applying morphological erosion to SAM3-generated masks (Carion et al., 2025), it constructs a hierarchy of interior regions to explicitly decouple boundary alignment errors from internal texture artifacts.

By operationalizing this hybrid protocol, we systematically decompose VTON quality into five orthogonal axes as illustrated in Figure 1. Specifically, we assess *background consistency* to strictly preserve non-editing regions, and *identity fidelity* to maintain the subject’s facial and bodily characteristics. Furthermore, we examine *texture fidelity* and *shape plausibility* to ensure both high-frequency pattern retention and physically natural warping, culminating in *overall realism* which gauges the holistic perceptual harmony of the composite. This five-axis taxonomy serves as the theoretical backbone of our benchmark. Together, these dimensions bridge the gap between semantic correctness and structural integrity, enabling a granular and interpretable diagnosis of VTON deficiencies that transcends coarse holistic scoring. Our contributions are summarized as follows:

- **OpenVTON-Bench:** We release a commercial-grade benchmark constructed from **~100K high-resolution image pairs** at resolutions up to 1536², which are processed into **standardized triplets** featuring rich semantic annotations and balanced categories to overcome prior limitations.
- **Hybrid Evaluation Paradigm:** We establish a new standard by integrating **VLM-as-a-Judge** for semantic reasoning with a **Multi-Scale Representation Metric** for structural verification. This hybrid approach correlates better with human judgment.
- **Diagnostic Analysis:** Benchmarking state-of-the-art models reveals that while modern diffusion models excel in photorealism, they frequently fail in fine-grained texture preservation—a critical insight revealed only through our dual-track evaluation.

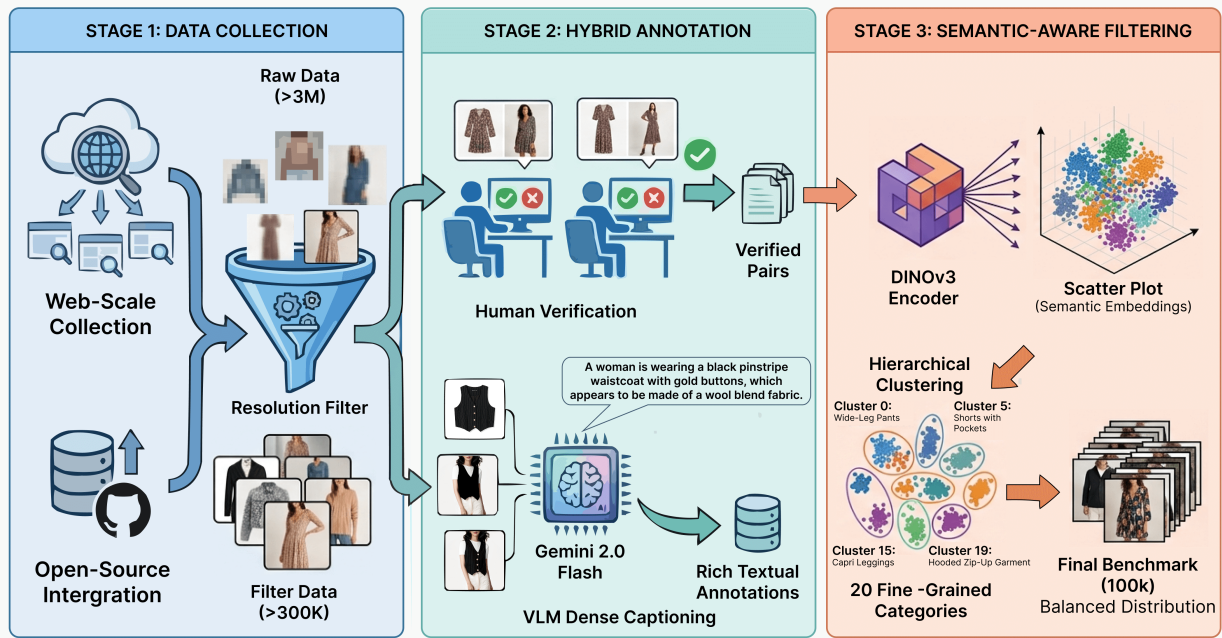


Figure 2. **Data Construction Pipeline of OpenVTON-Bench.** The process consists of three stages: (1) Large-scale raw data aggregation from diverse sources; (2) Hybrid annotation combining human verification for pair alignment and VLM-based dense captioning; (3) Semantic-aware filtering using DINOv3 clustering to ensure a balanced distribution across 20 fine-grained categories.

2. OpenVTON-Bench

Constructing a benchmark that accurately reflects the demands of commercial virtual try-on requires moving beyond simple studio settings. In this section, we detail the construction pipeline of **OpenVTON-Bench**, covering data acquisition, hybrid annotation, semantic-aware filtering, and detailed statistics. The overall construction pipeline is illustrated in Figure 2.

2.1. Data Collection

To ensure diversity in body shapes, poses, and clothing styles, we aggregated data from two primary streams, targeting a minimum resolution of 1024×1024 :

- Open-Source Integration:** We curated high-quality subsets from existing datasets, filtering for samples that meet our resolution threshold (Shen et al., 2024).
- Web-Scale Collection:** We collected images from publicly available online sources following standard practices in benchmark construction (Schuhmann et al., 2021). In contrast to academic datasets captured under controlled conditions, these images reflect real-world variability, including diverse lighting, poses, and backgrounds. The dataset will be released under a strict research-only license that prohibits commercial use. To respect intellectual property rights, we provide a takedown mechanism allowing copyright holders to re-

quest prompt removal of specific samples. All personally identifiable information is anonymized to ensure privacy compliance.

The initial raw collection exceeded **3,000,000** samples. We applied a strict resolution constraint, retaining only images whose *height and width are at least 1024 pixels*, while *the longer side does not exceed 1536 pixels*. This criterion allows both square and rectangular images, and ensures that all retained samples satisfy the high-fidelity requirements of modern commercial VTON applications. After this filtering stage, approximately 300,000 samples remained. The final 99,925 images were obtained through a subsequent stratified sampling process (Section 2.3).

2.2. Hybrid Annotation Pipeline

High-quality VTON requires not only precise image pairs but also rich semantic context. We employed a Human-AI hybrid annotation strategy.

Human-in-the-Loop Pair Verification. The core of VTON datasets is the correspondence between the *in-shop garment* (source) and the *person wearing it* (reference). Automated matching often fails with complex layering. We deployed annotators to verify all candidate pairs in the 300K pool, discarding samples with mismatched items, severe occlusions, or missing views.

VLM-Powered Dense Captioning. To support text-guided

editing and multimodal evaluation, we utilized Gemini 2.0 Flash (Team, 2025)—selected for its strong performance on fine-grained visual attribute extraction and cost efficiency at scale—to generate comprehensive descriptions for each garment. To enhance the precision of these descriptions, we implemented a hierarchical prompting strategy.

This process begins with a coarse-grained classification prompt that categorizes the primary garment in an image as either an ‘upper-body’ or ‘lower-body’ item. For this initial sort, full-body garments such as dresses are classified as upper-body items that we found to produce more coherent captions. Following this classification, a specialized prompt is conditionally applied. For upper-body garments, the VLM is guided to extract *Structure* (sleeve length, neckline), *Texture* (fabric, patterns), and *Design Details* (logos, ruffles), while for lower-body garments, the focus shifts to analogous details such as *Structure* (fit, cut), *Texture* (denim, wash), and *Design Details* (pockets, embroidery).

This two-tiered methodology ensures that the extracted attributes are contextually relevant, generating rich textual annotations that far exceed the granularity of traditional, monolithic label-based systems.

2.3. Semantic-Aware Filtering via DINOv3

A challenge in fashion datasets is the long-tail distribution problem—simple items like “white t-shirts” often dominate, while complex textures are underrepresented. To construct a balanced benchmark, we implemented a semantic clustering pipeline utilizing Self-Supervised Learning (SSL).

Semantic Embedding Extraction. We fed all verified garment images into the **DINOv3 (ViT-H+)** (Siméoni et al., 2025) encoder. DINOv3 was selected for its superior ability to capture holistic semantic structures and object-level features compared to CLIP, which focuses more on text alignment. This yields a robust visual representation invariant to slight deformations.

Hierarchical Clustering & Stratified Sampling. We performed hierarchical clustering on the extracted embeddings, categorizing the dataset into **20 fine-grained classes** (e.g., *Cropped Knit Tops*, *Button-Front Coats*, *Wide-Leg Pants*). From an initial pool of approximately 300,000 candidates, we applied stratified sampling based on these clusters to curate the final **99,925** samples. Although this count is slightly below the integer threshold, we designate this balanced version as the “**100K**” dataset for terminological convenience. This sampling strategy explicitly down-samples over-represented categories and retains high-complexity samples, challenging models to generalize across diverse textures and topologies rather than overfitting to simple patterns. The t-SNE visualization of the dataset distributions is shown in Figure 3.

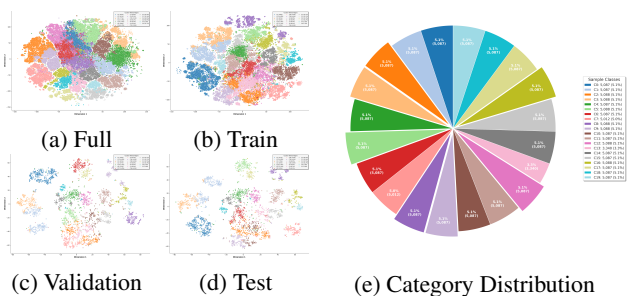


Figure 3. **Dataset Analysis of OpenVTON-Bench.** Left (a-d): t-SNE visualizations of the full dataset and the train/validation/test splits. Right (e): Category distribution of the dataset.

2.4. Benchmark Overview and Statistics

The final OpenVTON-Bench comprises 99,925 high-resolution image pairs, establishing itself as one of the largest VTON benchmarks with consistent high fidelity. As summarized in Table 1, OpenVTON-Bench maintains a minimum resolution of 1024×1024 , with images reaching up to 1536×1536 —a critical requirement for evaluating the fine-grained texture generation capabilities of modern diffusion-based models.

Beyond scale, OpenVTON-Bench provides substantially richer annotations than its predecessors. Each sample is accompanied by dense semantic captions totaling over 3 million words, capturing nuanced attributes such as fabric texture, pattern complexity, and design details that are absent from traditional label-based annotations. This enables not only more comprehensive evaluation but also opens avenues for text-guided VTON research.

Finally, Figure 3 presents the category distribution of the training, validation, and test splits over the 20 garment categories. The similar distributions across splits indicate that our dataset partitioning preserves category balance, reducing evaluation bias and enabling reliable comparison across different VTON models. Figure 4 further illustrates some samples from OpenVTON-Bench, highlighting the diversity of garment types, poses, and visual appearances. Additional visualizations and large-scale examples are provided in Appendix D.3.

3. Evaluation Protocol

To rigorously assess the quality of virtual try-on synthesis, we propose a multi-modal evaluation protocol that goes beyond traditional pixel-wise comparisons. Our protocol integrates semantic reasoning from Vision-Language Models (VLMs), hierarchical feature analysis from self-supervised learning representations, and conventional statistical metrics, enabling a comprehensive and fine-grained evaluation.



Figure 4. Representative examples from OpenVTON-Bench. More examples are provided in Appendix D.3.

3.1. Preliminaries and Notation

Let $\mathcal{D} = \{(I_p, I_g, I_{gt})\}$ denote the evaluation dataset, where I_p is the cloth-agnostic person image, I_g is the target garment image, and I_{gt} is the ground-truth try-on result. A virtual try-on model G produces a synthesized image as defined in Eq. 1.

$$\hat{I} = G(I_p, I_g), \quad (1)$$

The generated image \hat{I} is evaluated against I_{gt} . We denote by $\Phi(\cdot)$ a frozen SSL image encoder and by $\mathcal{SAM}(\cdot)$ a frozen segmentation foundation model used for garment localization. The overall evaluation space is defined as $\mathcal{E} = \{\mathcal{E}_{\text{VLM}}, \mathcal{E}_{\text{Rep}}, \mathcal{E}_{\text{Pix}}\}$, corresponding to semantic-, representation-, and pixel-level metrics, respectively.

3.2. Objective Evaluation

3.2.1. VLM-BASED SEMANTIC SCORING

Human perception of realism primarily depends on high-level semantic consistency. To capture this, we employ a Vision-Language Model (Qwen-VL-Plus (Bai et al., 2025)) as a surrogate perceptual judge. For each test case, the model evaluates a visual triplet (I_g, I_{gt}, \hat{I}) —where \hat{I} replaces the masked input—together with a task-specific prompt \mathcal{T} and outputs a five-dimensional semantic score vector as formulated in Eq. 2.

$$\mathbf{s} = [s_{bg}, s_{id}, s_{tex}, s_{shape}, s_{real}] = \mathcal{V}(I_g, I_{gt}, \hat{I}; \mathcal{T}), \quad (2)$$

Each scalar score lies in $[1, 5]$ and corresponds to background consistency, identity preservation, texture fidelity, shape preservation, and overall realism, respectively. This formulation allows the evaluation of semantic attributes (e.g., logo clarity or garment-category correctness) that are not accessible to conventional CNN-based metrics.

3.2.2. REPRESENTATION-BASED METRICS

Pixel-level distances are overly sensitive to minor spatial misalignments that are perceptually negligible. To robustly assess identity preservation and garment texture fidelity,

we introduce representation-based metrics built upon DINOv3 (Siméoni et al., 2025) features and mask guidance from SAM3 (Carion et al., 2025).

Global Identity Consistency. Overall visual coherence is evaluated by computing the cosine similarity between global image embeddings extracted by $\Phi(\cdot)$. Specifically, the global identity consistency score is defined as

$$S_{\text{global}}(\hat{I}, I_{gt}) = \frac{\Phi(\hat{I})^\top \Phi(I_{gt})}{\|\Phi(\hat{I})\|_2 \|\Phi(I_{gt})\|_2}, \quad (3)$$

where Eq. 3 measures the alignment between the generated image and the ground truth in the global feature space. A higher S_{global} indicates better preservation of person identity and overall structural coherence.

Multi-scale Garment Fidelity. To disentangle boundary misalignment from internal texture distortion, we further propose a mask-guided multi-scale garment evaluation. First, a binary garment mask is extracted from the ground-truth image as defined in Eq. 4.

$$M_{gt} = \mathcal{SAM}(I_{gt}). \quad (4)$$

Similarly, we apply the same segmentation process to the generated image \hat{I} to obtain its corresponding mask \hat{M} . Based on these masks, we generate sets of K nested masks by progressive morphological erosion. Given a structural element B , the k -th eroded mask is defined as:

$$M_*^{(k)} = M_* \ominus \underbrace{(B \oplus \dots \oplus B)}_{k \text{ times}}, \quad (5)$$

where M_* denotes either M_{gt} or \hat{M} , and \ominus and \oplus denote erosion and dilation, respectively. As described in Eq. 5, smaller values of k retain garment boundary regions, while larger values focus on the interior fabric area.

For each scale k , we compute a masked feature similarity score in the SSL feature space:

$$S_{\text{rep}}^{(k)} = \frac{\Phi(\hat{I} \odot \hat{M}^{(k)})^\top \Phi(I_{gt} \odot M_{gt}^{(k)})}{\|\Phi(\hat{I} \odot \hat{M}^{(k)})\|_2 \|\Phi(I_{gt} \odot M_{gt}^{(k)})\|_2}, \quad (6)$$

where \odot denotes element-wise multiplication. According to Eq. 6, a higher $S_{\text{rep}}^{(k)}$ reflects better garment texture fidelity at the corresponding spatial scale, enabling fine-grained diagnosis of boundary versus interior errors.

3.2.3. PIXEL-BASED STATISTICAL METRICS

For completeness and compatibility with prior benchmarks, we additionally report conventional pixel-level and distribution-based metrics, including PSNR, SSIM, LPIPS, and FID (Hore & Ziou, 2010; Detlefsen et al., 2022; Zhang et al., 2018; Heusel et al., 2017). These metrics are treated as auxiliary references, and their limitations in capturing perceptual and semantic fidelity are discussed in Sec. 1.



Figure 5. Qualitative comparison of state-of-the-art methods on OpenVTON-Bench.

3.3. Subjective Evaluation

To validate the reliability of the proposed objective metrics, we conduct a large-scale human perceptual study. A total of 76 participants provided over 90,000 valid ratings by evaluating randomly sampled result triplets (I_g, I_{gt}, \hat{I}) . In each triplet, \hat{I} represents the VTON result generated from the corresponding masked input according to Eq. 1. Each image was scored on a five-point Likert scale along the same five semantic dimensions defined in Eq. 2. To ensure the fairness of the assessment, we ensured that each group of images was evaluated at least twice and the average score was used. The aggregated human scores are treated as perceptual ground truth, and we compute the Pearson correlation coefficient r between human judgments and each objective metric to quantify their alignment with human perception.

4. Experimental Results

In this section, we conduct a comprehensive benchmarking of state-of-the-art virtual try-on systems on OpenVTON-Bench. We evaluate **nine** representative methods, covering both diffusion-based paradigms and editing-based frameworks. Our analysis aims to answer two fundamental questions: (1) How well do current models handle the fine-grained semantic and texture challenges proposed in our dataset? (2) How effectively do our proposed evaluation metrics align with human perception compared to traditional protocols?

4.1. Semantic and Perceptual Evaluation

We first assess the semantic alignment and realism using our VLM-based evaluation protocol (S_{VLM}) and Human Evaluation (S_{Human}). As reported in Table 2, we make the following observations:

VLM Agents as Reliable Judges. The scores assigned by our VLM-based metric closely mirror the human ratings across most dimensions. Notably, **YingHui** achieves the highest scores in both VLM ($S_{avg} = 4.372$) and Human evaluation ($S_{avg} = 4.608$). This consistency suggests that Multimodal LLMs utilize semantic understanding similar to human cognition when assessing “Realism” and “Iden-

tity,” making them a scalable alternative to costly manual annotation.

The “Texture-Realism” Gap. A critical trend is observed in the *Texture* dimension (S_{tex}). While general-purpose diffusion models like FLUX.1-Kontext-dev achieve high scores in *Background* (4.428) and *Realism* (4.137), their performance drops significantly in *Texture* (3.574). This indicates that while large-scale pre-training yields photorealism, it struggles with the zero-shot preservation of specific garment patterns. Models explicitly trained or fine-tuned on high-quality try-on data (e.g., YingHui, HuiWa) exhibit a much balanced performance profile, verifying the necessity of domain-specific benchmarks like OpenVTON-Bench.

4.2. Fine-Grained Texture Fidelity

Pixel-based metrics often fail to distinguish between correct texture synthesis and mere boundary alignment. To address this, we employ our Representation-based Similarity (S_{rep}) with progressive mask erosion, which forces the evaluation to focus on the *inner* garment details rather than edge contrast. The results are presented in Table 3.

Robustness to Erosion. A decreasing trend in similarity scores is observed for all methods as the mask erodes. However, the rate of decay varies. OOTD drops significantly from 0.797 to 0.669 ($\Delta \approx 0.13$), implying its high scores rely partly on boundary correctness. It is also worth noting the foundational leap between generations: FLUX.2-dev significantly outperforms FLUX.1-Kontext-dev across all levels ($\bar{S}_{rep} : 0.841$ vs. 0.754), underscoring the critical role of a strong generative backbone in preserving high-frequency details. In contrast, YingHui maintains high fidelity even at the deepest erosion level ($S_{rep}^{(3)} = 0.823$), demonstrating that it learns valid internal texture representations.

Global & Local Consistency. While Nanobanana and Qwen-Editor achieve competitive scores in global consistency ($S_{global} = 0.936$), YingHui consistently outperforms them in local garment similarity ($\bar{S}_{rep} = 0.864$). This highlights the limitation of using whole-image embeddings for try-on assessment: a model can generate a visually pleasing image (high global score) while failing to preserve the specific details of the merchandise (lower local score).

Table 2. Semantic Evaluation via VLM and Human Annotators. We report the scores (scale 1–5) across five semantic dimensions: Background (s_{bg}), Identity (s_{id}), Texture (s_{tex}), Shape (s_{shape}), and Overall Realism (s_{real}). **Bold** indicates the best result, and underline indicates the second best.

Method	s_{bg}		s_{id}		s_{tex}		s_{shape}		s_{real}		s_{avg}	
	VLM	Human	VLM	Human	VLM	Human	VLM	Human	VLM	Human	VLM	Human
OOTD (Xu et al., 2025)	4.074	4.608	3.685	3.832	3.278	3.217	3.898	3.697	3.794	3.595	3.746	3.790
UNO (Wu et al., 2025b)	4.167	3.220	3.749	2.308	3.577	2.364	4.141	2.907	4.067	3.913	3.940	2.942
EasyControl (Zhang et al., 2025)	4.273	4.459	3.824	3.496	3.506	3.163	4.105	3.824	4.055	3.900	3.953	3.768
FLUX.1-Kontext-dev (Labs et al., 2025)	4.428	4.406	3.957	3.535	3.574	3.122	4.158	3.768	4.137	4.060	4.051	3.778
FLUX.2-dev (Labs, 2025)	4.593	<u>4.734</u>	4.226	4.460	4.007	3.914	4.446	4.494	4.409	4.582	4.336	4.437
Nanobanana (Google DeepMind, 2025)	4.610	4.722	4.253	4.689	4.019	<u>4.225</u>	4.457	<u>4.646</u>	4.418	4.694	4.351	<u>4.595</u>
Qwen-Editor (Wu et al., 2025a)	<u>4.617</u>	4.729	<u>4.270</u>	4.606	<u>4.046</u>	<u>4.132</u>	<u>4.472</u>	4.590	<u>4.431</u>	4.666	<u>4.367</u>	4.545
HuiWa (Creative & Platform, 2024)	4.611	4.682	4.256	4.538	4.050	4.018	4.465	4.546	4.424	4.664	4.361	4.490
YingHui (Platform, 2025)	4.624	4.735	4.277	<u>4.685</u>	4.050	4.252	4.473	4.675	4.437	<u>4.693</u>	4.372	4.608

Table 3. Representation-based Similarity Evaluation. S_{global} measures holistic semantic consistency. $S_{rep}^{(k)}$ denotes garment-level similarity under increasing mask erosion levels ($0 \rightarrow 3$), isolating texture quality from boundary artifacts.

Method	S_{global}	$S_{rep}^{(0)}$	$S_{rep}^{(1)}$	$S_{rep}^{(2)}$	$S_{rep}^{(3)}$	\bar{S}_{rep}	\bar{S}
OOTD (Xu et al., 2025)	0.844	0.797	0.755	0.701	0.669	0.731	0.788
EasyControl (Zhang et al., 2025)	0.854	0.830	0.807	0.765	0.729	0.783	0.818
UNO (Wu et al., 2025b)	0.737	0.763	0.730	0.674	0.628	0.699	0.718
FLUX.1-Kontext-dev (Labs et al., 2025)	0.849	0.813	0.778	0.731	0.694	0.754	0.802
FLUX.2-dev (Labs, 2025)	0.928	0.886	0.863	0.823	0.793	0.841	0.885
NanobananaPro (Google DeepMind, 2025)	0.936	0.894	0.865	0.827	0.807	0.848	0.892
Qwen-Editor (Wu et al., 2025a)	0.936	0.903	0.876	0.840	0.819	0.859	<u>0.898</u>
HuiWa (Creative & Platform, 2024)	<u>0.933</u>	0.882	0.859	0.821	0.793	0.839	0.886
YingHui (Platform, 2025)	0.936	0.904	0.882	0.847	0.823	0.864	0.900

Consequently, judging by the aggregated metric \bar{S} , modern commercial-grade systems have effectively bridged the gap between semantic coherence and pixel-level fidelity, leaving earlier open-source attempts (e.g., UNO, OOTD) distinctly behind.

4.3. Pixel-based Metrics and Correlation Analysis

Finally, we report standard pixel-level metrics (PSNR, SSIM, LPIPS, FID) in Table 4 and conduct a meta-evaluation of all metrics against human judgment in Table 5.

Saturation of Traditional Metrics. In Table 4, **Qwen-Editor** achieves the best scores in PSNR (26.343) and SSIM (0.905). However, visual inspection suggests that it often minimizes pixel-wise error by smoothing textures. Conversely, **YingHui** achieves the best FID (7.372), indicating superior distribution-level realism. The discrepancy between high PSNR and lower perceptual quality underscores the limitations of pixel-wise metrics for generative tasks.

Meta-Evaluation: Ranking Consistency. To validate the reliability of OpenVTON-Bench, we analyze the correlation with human preference using three coefficients: Spearman (ρ_s) for ranking, Pearson (ρ_p) for linearity, and notably Kendall’s Tau (ρ_k) for pairwise ordering consistency. As shown in Table 5 and visualized in Figure 6, our **Representation Metric** (\bar{S}) dominates in ranking capabilities, achieving the highest ρ_k (0.833) and ρ_s (0.933). The high ρ_k score is particularly significant for a benchmark, as it indicates

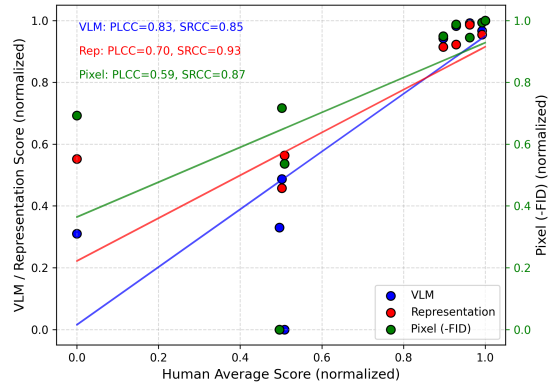


Figure 6. Correlation Analysis against Human Preference. The scatter plot compares objective metrics (normalized) with human ratings. Our **Representation Metric** (Red) and **VLM Metric** (Blue) show strong positive correlations.

that for any given pair of models, our metric is the most likely to correctly predict which one a human would prefer, far exceeding standard metrics like SSIM ($\rho_k = 0.611$).

5. Related Works

5.1. Virtual Try-On: Methods and Benchmarks

The evolution of Virtual Try-On (VTON) has transitioned from warping-based synthesis to generative modeling. Early GAN-based methods (Han et al., 2018; Wang et al., 2018; Honda, 2019; Lewis et al., 2021; Choi et al., 2021b; Isenbuth et al., 2020; Ge et al., 2021; Lee et al., 2022) relied on explicit cloth warping (Duchon, 2006; Jaderberg et al., 2015; Li et al., 2019), which often fails to handle complex poses or high resolutions due to geometric limitations. Conversely, recent diffusion-based approaches (Morelli et al., 2023; Zhu et al., 2023; Zheng et al., 2024; Shim et al., 2024; Kim et al., 2024; Zeng et al., 2024; Chong et al., 2024; Sun et al., 2025; Chong et al., 2025; Kim et al., 2025) formulate VTON as conditional inpainting, significantly improving photorealism and non-rigid deformation handling. However,

Table 4. Pixel-based Evaluation. While Qwen-Editor dominates in pixel-alignment metrics (PSNR/SSIM), YingHui achieves the best FID, indicating superior distribution-level realism. \uparrow denotes higher is better; \downarrow denotes lower is better.

Method	PSNR \uparrow	SSIM \uparrow	LPIPS \downarrow	FID \downarrow
OOTD (Xu et al., 2025)	16.534	0.794	0.255	55.216
EasyControl (Zhang et al., 2025)	15.731	0.779	0.277	39.079
UNO (Wu et al., 2025b)	12.096	0.726	0.417	110.534
FLUX.1-Kontext-dev (Labs et al., 2025)	15.389	0.747	0.280	36.555
FLUX.2-dev (Labs, 2025)	22.884	0.873	0.117	12.562
NanobananaPro (Google DeepMind, 2025)	<u>24.681</u>	<u>0.890</u>	<u>0.089</u>	<u>7.989</u>
Qwen-Editor (Wu et al., 2025a)	26.343	0.905	0.082	13.037
HuiWa (Creative & Platform, 2024)	23.045	0.875	0.100	8.619
YingHui (Platform, 2025)	22.593	0.870	0.101	7.372

Table 5. Meta-Evaluation: Correlation with Human Judgment. Our proposed metrics align significantly better with human preference. Notably, \mathcal{S} achieves the highest Kendall’s Tau (ρ_k), indicating superior pairwise ranking accuracy.

Metric	$\rho_s \uparrow$	$\rho_k \uparrow$	$\rho_p \uparrow$
s_{avg} (VLM)	0.850	<u>0.722</u>	0.828
\mathcal{S} (Rep)	0.933	0.833	0.701
PSNR	0.767	0.611	<u>0.819</u>
SSIM	0.767	0.611	0.801
–LPIPS	0.833	0.667	0.782
–FID	<u>0.867</u>	<u>0.722</u>	0.588

despite these architectural gains, a critical *data bottleneck* persists: models struggle with misalignment at resolutions beyond 1K due to the scarcity of high-quality training data.

Existing benchmarks struggle to balance supervision quality with environmental diversity. Controlled paired datasets (Dong et al., 2019; Choi et al., 2021a; Morelli et al., 2022) offer reliable ground truth but lack pose and background variation, whereas in-the-wild collections (Liu et al., 2016; Xie et al., 2021; Feng et al., 2022; Cui et al., 2024; Fu et al., 2022; Li et al., 2024b) provide realism but lack paired supervision, complicating faithful evaluation. Although recent efforts like VTONQA (Wei et al., 2026) and VTBench (Xiaobin et al., 2025) explore higher resolutions and refined metrics, they remain constrained by limited scale, instability from model-generated hallucinations, or closed-source policies. To address these limitations, we introduce OpenVTON-Bench, a large-scale ($\sim 100K$), high-resolution (1.5K) benchmark that uniquely combines paired supervision with in-the-wild diversity, enabling rigorous evaluation of next-generation systems.

5.2. Evaluation Protocols: From Pixels to Semantics

Evaluating virtual try-on quality is inherently challenging, as it requires simultaneously preserving garment fidelity and ensuring realistic integration with the person. Conventional protocols rely on pixel-level metrics (e.g., SSIM (Detlefsen et al., 2022), PSNR (Hore & Ziou, 2010)) and distribution-based distances (e.g., FID (Heusel et al.,

2017), LPIPS (Zhang et al., 2018)). However, these metrics are poorly aligned with high-fidelity try-on: pixel-wise scores penalize legitimate spatial variations, while FID captures global statistics but overlooks instance-level errors such as distorted textures or incorrect patterns. Recent efforts move toward semantic-aware evaluation. CLIP-based scores (Song et al., 2024) offer coarse semantic alignment but lack sensitivity to fine-grained fashion details. With the rise of VLMs (Zhu et al., 2025; Comanici et al., 2025; Li et al., 2024a; Bai et al., 2025; Lu et al., 2025), the *VLM-as-a-Judge* paradigm (Chen et al., 2024; Lin et al., 2025) enables human-like semantic assessment, yet remains susceptible to prompt bias and hallucination. We propose a hybrid protocol combining VLM-based semantics and DINOv3 features to robustly evaluate texture fidelity under non-rigid deformations, offering a more human-aligned VTON assessment.

6. Conclusion

In this paper, we introduce **OpenVTON-Bench**, a commercial-grade benchmark designed to bridge the gap between generative capability and rigorous evaluation in Virtual Try-On. By leveraging DINOv3-based semantic clustering and Gemini-powered dense captioning, we construct 100K high-resolution (1.5K) pairs that effectively mitigate the “studio-centric bias” of prior works. We further establish a hybrid evaluation protocol combining VLM semantic reasoning with a structure-aware Multi-Scale Representation Metric. Our benchmarking reveals a notable “texture-realism gap” in state-of-the-art diffusion models: while photorealistic, they often hallucinate fine-grained garment details—a nuance our metric disentangles more effectively than traditional pixel-level measures.

Limitations. Despite these contributions, several limitations remain. First, our pipeline relies on off-the-shelf foundation models (e.g., Gemini, DINOv3) for data filtering and captioning; while efficient, this may inevitably introduce minor semantic biases or hallucinations inherited from the upstream models. Second, although we significantly increased resolution to 1.5K, extreme cases involving complex multi-layer occlusions or acrobatic poses are still under-represented compared to standard studio poses. Future iterations will focus on refining these automated annotations and expanding topological diversity. We will make the data and code publicly available, hoping OpenVTON-Bench serves as a reliable compass guiding the community toward VTON systems that achieve not only visual plausibility but also strict commercial fidelity.

References

Bai, J., Bai, S., Yang, S., Wang, S., Tan, S., Wang, P., Lin, J., Zhou, C., and Zhou, J. Qwen-vl: A versatile vision-

- language model for understanding, localization, text reading, and beyond. *arXiv preprint arXiv:2308.12966*, 2023.
- Bai, S., Chen, K., Liu, X., Wang, J., Ge, W., Song, S., Dang, K., Wang, P., Wang, S., Tang, J., et al. Qwen2. 5-vl technical report. *arXiv preprint arXiv:2502.13923*, 2025.
- Carion, N., Gustafson, L., Hu, Y.-T., Debnath, S., Hu, R., Suris, D., Ryali, C., Alwala, K. V., Khedr, H., Huang, A., Lei, J., Ma, T., Guo, B., Kalla, A., Marks, M., Greer, J., Wang, M., Sun, P., Rädle, R., Afouras, T., Mavroudi, E., Xu, K., Wu, T.-H., Zhou, Y., Momeni, L., Hazra, R., Ding, S., Vaze, S., Porcher, F., Li, F., Li, S., Kamath, A., Cheng, H. K., Dollár, P., Ravi, N., Saenko, K., Zhang, P., and Feichtenhofer, C. Sam 3: Segment anything with concepts, 2025. URL <https://arxiv.org/abs/2511.16719>.
- Chen, D., Chen, R., Zhang, S., Wang, Y., Liu, Y., Zhou, H., Zhang, Q., Wan, Y., Zhou, P., and Sun, L. Mllm-as-a-judge: Assessing multimodal llm-as-a-judge with vision-language benchmark. In *Forty-first International Conference on Machine Learning*, 2024.
- Choi, S., Park, S., Lee, M., and Choo, J. Viton-hd: High-resolution virtual try-on via misalignment-aware normalization, 2021a. URL <https://arxiv.org/abs/2103.16874>.
- Choi, S., Park, S., Lee, M., and Choo, J. Viton-hd: High-resolution virtual try-on via misalignment-aware normalization. In *Proceedings of the IEEE/CVF conference on computer vision and pattern recognition*, pp. 14131–14140, 2021b.
- Chong, Z., Dong, X., Li, H., Zhang, S., Zhang, W., Zhang, X., Zhao, H., Jiang, D., and Liang, X. Catvton: Concatenation is all you need for virtual try-on with diffusion models. *arXiv preprint arXiv:2407.15886*, 2024.
- Chong, Z., Zhang, W., Zhang, S., Zheng, J., Dong, X., Li, H., Wu, Y., Jiang, D., and Liang, X. Catv2ton: Taming diffusion transformers for vision-based virtual try-on with temporal concatenation. *arXiv preprint arXiv:2501.11325*, 2025.
- Comanici, G., Bieber, E., Schaekermann, M., Pasupat, I., Sachdeva, N., Dhillon, I., Blistein, M., Ram, O., Zhang, D., Rosen, E., et al. Gemini 2.5: Pushing the frontier with advanced reasoning, multimodality, long context, and next generation agentic capabilities. *arXiv preprint arXiv:2507.06261*, 2025.
- Creative, H. A. and Platform, M. Huiwa ai creative and marketing platform, 2024. URL <https://www.ihuiwa.com/>.
- Cui, A., Mahajan, J., Shah, V., Gomathinayagam, P., Liu, C., and Lazebnik, S. Street tryon: Learning in-the-wild virtual try-on from unpaired person images. In *Proceedings of the IEEE/CVF Conference on Computer Vision and Pattern Recognition*, pp. 8235–8239, 2024.
- Detlefsen, N. S., Borovec, J., Schock, J., Jha, A. H., Koker, T., Di Liello, L., Stancl, D., Quan, C., Grechkin, M., and Falcon, W. Torchmetrics-measuring reproducibility in pytorch. *Journal of Open Source Software*, 7(70):4101, 2022.
- Dong, H., Liang, X., Wang, B., Lai, H., Zhu, J., and Yin, J. Towards multi-pose guided virtual try-on network, 2019. URL <https://arxiv.org/abs/1902.11026>.
- Duchon, J. Splines minimizing rotation-invariant seminorms in sobolev spaces. In *Constructive theory of functions of several variables: proceedings of a conference held at oberwolfach April 25–May 1, 1976*, pp. 85–100. Springer, 2006.
- Feng, R., Ma, C., Shen, C., Gao, X., Liu, Z., Li, X., Ou, K., Zhao, D., and Zha, Z.-J. Weakly supervised high-fidelity clothing model generation. In *Proceedings of the IEEE/CVF conference on computer vision and pattern recognition*, pp. 3440–3449, 2022.
- Fu, J., Li, S., Jiang, Y., Lin, K.-Y., Qian, C., Loy, C. C., Wu, W., and Liu, Z. Stylegan-human: A data-centric odyssey of human generation, 2022. URL <https://arxiv.org/abs/2204.11823>.
- Ge, C., Song, Y., Ge, Y., Yang, H., Liu, W., and Luo, P. Disentangled cycle consistency for highly-realistic virtual try-on. In *Proceedings of the IEEE/CVF conference on computer vision and pattern recognition*, pp. 16928–16937, 2021.
- Google DeepMind. Gemini 3 pro image model card. Technical report, Google, 2025. URL <https://storage.googleapis.com/deepmind-media/Model-Cards/Gemini-3-Pro-Image-Model-Card.pdf>.
- Han, X., Wu, Z., Wu, Z., Yu, R., and Davis, L. S. Viton: An image-based virtual try-on network, 2018. URL <https://arxiv.org/abs/1711.08447>.
- Heusel, M., Ramsauer, H., Unterthiner, T., Nessler, B., and Hochreiter, S. Gans trained by a two time-scale update rule converge to a local nash equilibrium. *Advances in neural information processing systems*, 30, 2017.
- Honda, S. Viton-gan: Virtual try-on image generator trained with adversarial loss. *Eurographics 2019 - Posters*, 2019. doi: 10.2312/EGP.20191043. URL <https://diglib.org/handle/10.2312/egp20191043>.

- Hore, A. and Ziou, D. Image quality metrics: Psnr vs. ssim. In *2010 20th international conference on pattern recognition*, pp. 2366–2369. IEEE, 2010.
- Issenhuth, T., Mary, J., and Calauzenes, C. Do not mask what you do not need to mask: a parser-free virtual try-on. In *European Conference on Computer Vision*, pp. 619–635. Springer, 2020.
- Jaderberg, M., Simonyan, K., Zisserman, A., et al. Spatial transformer networks. *Advances in neural information processing systems*, 28, 2015.
- Kim, J., Gu, G., Park, M., Park, S., and Choo, J. Stableviton: Learning semantic correspondence with latent diffusion model for virtual try-on. In *Proceedings of the IEEE/CVF conference on computer vision and pattern recognition*, pp. 8176–8185, 2024.
- Kim, J., Jin, H., Park, S., and Choo, J. Promptdresser: Improving the quality and controllability of virtual try-on via generative textual prompt and prompt-aware mask, 2025. URL <https://arxiv.org/abs/2412.16978>.
- Labs, B. F. FLUX.2: Frontier Visual Intelligence. <https://bfl.ai/blog/flux-2>, 2025.
- Labs, B. F., Batifol, S., Blattmann, A., Boesel, F., Consul, S., Diagne, C., Dockhorn, T., English, J., English, Z., Esser, P., Kulal, S., Lacey, K., Levi, Y., Li, C., Lorenz, D., Müller, J., Podell, D., Rombach, R., Saini, H., Sauer, A., and Smith, L. Flux.1 kontext: Flow matching for in-context image generation and editing in latent space, 2025. URL <https://arxiv.org/abs/2506.15742>.
- Lee, S., Gu, G., Park, S., Choi, S., and Choo, J. High-resolution virtual try-on with misalignment and occlusion-handled conditions. In *European Conference on Computer Vision*, pp. 204–219. Springer, 2022.
- Lewis, K. M., Varadharajan, S., and Kemelmacher-Shlizerman, I. Tryongan: Body-aware try-on via layered interpolation, 2021. URL <https://arxiv.org/abs/2101.02285>.
- Li, B., Zhang, Y., Guo, D., Zhang, R., Li, F., Zhang, H., Zhang, K., Zhang, P., Li, Y., Liu, Z., et al. Llava-onevision: Easy visual task transfer. *arXiv preprint arXiv:2408.03326*, 2024a.
- Li, N., Liu, Q., Singh, K. K., Wang, Y., Zhang, J., Plummer, B. A., and Lin, Z. Unihuman: A unified model for editing human images in the wild. In *Proceedings of the IEEE/CVF conference on computer vision and pattern recognition*, pp. 2039–2048, 2024b.
- Li, Y., Huang, C., and Loy, C. C. Dense intrinsic appearance flow for human pose transfer. In *Proceedings of the IEEE/CVF conference on computer vision and pattern recognition*, pp. 3693–3702, 2019.
- Lin, I. W., Hu, Y., Li, S. S., Geng, S., Koh, P. W., Zettlemoyer, L., Althoff, T., and Ghazvininejad, M. Self-improving vlm judges without human annotations. *arXiv preprint arXiv:2512.05145*, 2025.
- Liu, S., Zeng, Z., Ren, T., Li, F., Zhang, H., Yang, J., Li, C., Yang, J., Su, H., Zhu, J., et al. Grounding dino: Marrying dino with grounded pre-training for open-set object detection. *arXiv preprint arXiv:2303.05499*, 2023.
- Liu, Z., Luo, P., Qiu, S., Wang, X., and Tang, X. Deepfashion: Powering robust clothes recognition and retrieval with rich annotations. In *Proceedings of IEEE Conference on Computer Vision and Pattern Recognition (CVPR)*, 2016.
- Lu, S., Li, Y., Xia, Y., Hu, Y., Zhao, S., Ma, Y., Wei, Z., Li, Y., Duan, L., Zhao, J., et al. Ovis2. 5 technical report. *arXiv preprint arXiv:2508.11737*, 2025.
- Morelli, D., Fincato, M., Cornia, M., Landi, F., Cesari, F., and Cucchiara, R. Dress code: High-resolution multi-category virtual try-on, 2022. URL <https://arxiv.org/abs/2204.08532>.
- Morelli, D., Baldrati, A., Cartella, G., Cornia, M., Bertini, M., and Cucchiara, R. Ladi-vton: Latent diffusion textual-inversion enhanced virtual try-on. In *Proceedings of the 31st ACM international conference on multimedia*, pp. 8580–8589, 2023.
- Platform, Y. A. C. Yinghui ai creative platform, 2025. URL <https://www.yinghuigen.com/>.
- Schuhmann, C., Vencu, R., Beaumont, R., Kaczmarczyk, R., Mullis, C., Katta, A., Coombes, T., Jitsev, J., and Komatsuzaki, A. Laion-400m: Open dataset of clip-filtered 400 million image-text pairs, 2021. URL <https://arxiv.org/abs/2111.02114>.
- Shen, F., Jiang, X., He, X., Ye, H., Wang, C., Du, X., Li, Z., and Tang, J. Imagdressing-v1: Customizable virtual dressing, 2024. URL <https://arxiv.org/abs/2407.12705>.
- Shim, S.-H., Chung, J., and Heo, J.-P. Towards squeezing-averse virtual try-on via sequential deformation. In *Proceedings of the AAAI Conference on Artificial Intelligence*, volume 38, pp. 4856–4863, 2024.
- Siméoni, O., Vo, H. V., Seitzer, M., Baldassarre, F., Oquab, M., Jose, C., Khalidov, V., Szafraniec, M., Yi, S., Ramamonjisoa, M., Massa, F., Haziza, D., Wehrstedt, L., Wang, J., Darcet, T., Moutakanni, T., Sentana, L., Roberts, C., Vedaldi, A., Tolan, J., Brandt, J., Couprie, C., Mairal, J.,

- Jégou, H., Labatut, P., and Bojanowski, P. DINOv3, 2025. URL <https://arxiv.org/abs/2508.10104>.
- Song, D., Zhang, X., Zhou, J., Nie, W., Tong, R., Kankanhalli, M., and Liu, A.-A. Image-based virtual try-on: A survey, 2024. URL <https://arxiv.org/abs/2311.04811>.
- Sun, X., Hong, Y., Zhan, J., Lan, J., Zhu, H., Wang, W., Zhang, L., and Zhang, J. Ds-vton: High-quality virtual try-on via disentangled dual-scale generation. *arXiv preprint arXiv:2506.00908*, 2025.
- Team, G. Gemini: A family of highly capable multimodal models, 2025. URL <https://arxiv.org/abs/2312.11805>.
- Wang, B., Zheng, H., Liang, X., Chen, Y., Lin, L., and Yang, M. Toward characteristic-preserving image-based virtual try-on network, 2018. URL <https://arxiv.org/abs/1807.07688>.
- Wang, H., Zhang, Z., Di, D., Zhang, S., and Zuo, W. Mv-vton: Multi-view virtual try-on with diffusion models. In *Proceedings of the AAAI Conference on Artificial Intelligence*, volume 39, pp. 7682–7690, 2025.
- Wei, X., Wu, S., Xu, Z., Li, Y., Duan, H., Min, X., and Zhai, G. Vtonqa: A multi-dimensional quality assessment dataset for virtual try-on, 2026. URL <https://arxiv.org/abs/2601.02945>.
- Wu, C., Li, J., Zhou, J., Lin, J., Gao, K., Yan, K., ming Yin, S., Bai, S., Xu, X., Chen, Y., Chen, Y., Tang, Z., Zhang, Z., Wang, Z., Yang, A., Yu, B., Cheng, C., Liu, D., Li, D., Zhang, H., Meng, H., Wei, H., Ni, J., Chen, K., Cao, K., Peng, L., Qu, L., Wu, M., Wang, P., Yu, S., Wen, T., Feng, W., Xu, X., Wang, Y., Zhang, Y., Zhu, Y., Wu, Y., Cai, Y., and Liu, Z. Qwen-image technical report, 2025a. URL <https://arxiv.org/abs/2508.02324>.
- Wu, S., Huang, M., Wu, W., Cheng, Y., Ding, F., and He, Q. Less-to-more generalization: Unlocking more controllability by in-context generation. *arXiv preprint arXiv:2504.02160*, 2025b.
- Xiaobin, H., Yujie, L., Donghao, L., Xu, P., Jiangning, Z., Junwei, Z., Chengjie, W., and Yanwei, F. Vtbench: Comprehensive benchmark suite towards real-world virtual try-on models, 2025. URL <https://arxiv.org/abs/2505.19571>.
- Xie, Z., Huang, Z., Zhao, F., Dong, H., Kampffmeyer, M., and Liang, X. Towards scalable unpaired virtual try-on via patch-routed spatially-adaptive gan, 2021. URL <https://arxiv.org/abs/2111.10544>.
- Xu, Y., Gu, T., Chen, W., and Chen, A. Ootdiffusion: Outfitting fusion based latent diffusion for controllable virtual try-on. In *Proceedings of the AAAI Conference on Artificial Intelligence*, volume 39, pp. 8996–9004, 2025.
- Yang, X., Ding, C., Hong, Z., Huang, J., Tao, J., and Xu, X. Texture-preserving diffusion models for high-fidelity virtual try-on. In *Proceedings of the IEEE/CVF conference on computer vision and pattern recognition*, pp. 7017–7026, 2024.
- Yang, Z., Li, Y., He, S., Li, X., Xu, Y., Dong, J., and Du, Y. Omnivton: Training-free universal virtual try-on. In *Proceedings of the IEEE/CVF International Conference on Computer Vision*, pp. 16702–16711, 2025.
- Zeng, J., Song, D., Nie, W., Tian, H., Wang, T., and Liu, A.-A. Cat-dm: Controllable accelerated virtual try-on with diffusion model. In *Proceedings of the IEEE/CVF conference on computer vision and pattern recognition*, pp. 8372–8382, 2024.
- Zhang, R., Isola, P., Efros, A. A., Shechtman, E., and Wang, O. The unreasonable effectiveness of deep features as a perceptual metric. In *Proceedings of the IEEE conference on computer vision and pattern recognition*, pp. 586–595, 2018.
- Zhang, Y., Yuan, Y., Song, Y., Wang, H., and Liu, J. Easy-control: Adding efficient and flexible control for diffusion transformer. In *Proceedings of the IEEE/CVF International Conference on Computer Vision*, pp. 19513–19524, 2025.
- Zheng, J., Zhao, F., Xu, Y., Dong, X., and Liang, X. Viton-dit: Learning in-the-wild video try-on from human dance videos via diffusion transformers. *arXiv preprint arXiv:2405.18326*, 2024.
- Zheng, L., Chiang, W.-L., Sheng, Y., Zhuang, S., Wu, Z., Zhuang, Y., Lin, Z., Li, Z., Li, D., Xing, E., et al. Judging llm-as-a-judge with mt-bench and chatbot arena. *Advances in neural information processing systems*, 36: 46595–46623, 2023.
- Zhu, J., Wang, W., Chen, Z., Liu, Z., Ye, S., Gu, L., Tian, H., Duan, Y., Su, W., Shao, J., et al. Internv13: Exploring advanced training and test-time recipes for open-source multimodal models. *arXiv preprint arXiv:2504.10479*, 2025.
- Zhu, L., Yang, D., Zhu, T., Reda, F., Chan, W., Saharia, C., Norouzi, M., and Kemelmacher-Shlizerman, I. Tryon-diffusion: A tale of two unets. In *Proceedings of the IEEE/CVF conference on computer vision and pattern recognition*, pp. 4606–4615, 2023.

A. Details of Data Collection and Annotation

Our dataset construction process prioritizes high resolution, high fidelity, and semantic richness. The pipeline consists of three distinct stages: Multi-source Collection, Semantic Balancing, and Automated Mask Generation.

A.1. Data Sources and Candidate Pool Construction

We construct the initial pool from two primary streams to ensure diversity in both fashion styles and imaging conditions.

Stream A: Social Media Subset (Refined IG Pair Dataset). To capture high-aesthetic “in-the-wild” scenarios, we conducted a deep refinement based on the IG Pair Dataset from IMAGDressing-v1 (Shen et al., 2024).

- **Manual Cleaning:** We performed strict manual re-screening to enforce a “one-to-one” constraint (one garment image strictly corresponds to one model image), eliminating the redundancy of multiple poses for a single garment.
- **Outcome:** We curated approximately 30,000 high-quality pairs from this source.

Stream B: Large-scale E-Commerce Subset. To ensure categorical coverage, we constructed a corpus from major e-commerce platforms.

- **Collection & Filtering:** We deployed aesthetic scoring and face detection models during crawling to filter out low-quality or headless images. From over 3 million raw pairs, we retained the high-quality subset.
- **Human Verification:** A team of over 1,000 annotators verified that the standalone garment strictly matches the model’s outfit and that no critical body parts are truncated.

Integration and Resolution Filtering. After merging both streams, we applied a strict resolution filter, selecting only images between 1024×1024 and 1536×1536 . This resulted in a massive **high-quality candidate pool of over 300,000 pairs**.

A.2. Semantic Balancing and Final Selection

Directly using the candidate pool may lead to long-tail distribution issues. To construct a balanced benchmark, we implemented a feature-driven sampling strategy.

- **DINOv3 Clustering:** We utilized **DINOv3** (Siméoni et al., 2025) to extract semantic embeddings for the 300k+ candidate pairs and performed K-Means clustering to partition the data into 20 distinct semantic clusters.
- **Balanced Sampling:** To ensure uniformity across styles and poses, we performed balanced sampling from these 20 clusters. This process downsampled the candidate pool to a final curated set of exactly **99,925** image pairs, which constitutes the core of **OpenVTON-Bench**.

A.3. VLM-assisted Annotation and Mask Generation

The raw dataset consists of high-quality **image pairs**: a *Reference Garment* and a corresponding *Model Image* wearing that garment. To prepare these pairs for standard VTON training and evaluation, we extended them into **triplets** by generating occlusion masks. **Fine-grained Categorization.** We employed **Qwen-VL-Plus** (Bai et al., 2023) to determine the specific clothing category for each of the 20 clusters. By sampling three representative images per cluster, the VLM provided precise semantic definitions, ensuring accurate categorization. **Automated Triplet Construction.** Finally, we formulated the training triplets (I_g, I_{gt}, I_m)—representing the Reference Garment, the Ground-Truth Model, and the Masked Model, respectively—using an automated pipeline:

- **Segmentation:** Using the category labels as prompts, **GroundingDINO** (Liu et al., 2023) detected the garment regions, and **SAM3** (Carion et al., 2025) generated precise pixel-level boundaries.

- **Occlusion (Mask Generation):** Based on the segmentation, we applied a black occlusion layer to the garment region of the original model image. We designate this occluded image as the **Masked Model** (I_m).

Consequently, the final dataset contains 99,925 triplets. During training, the generative model utilizes the pair of the Reference Garment (I_g) and the Masked Model (I_m) as inputs to reconstruct the target Ground-Truth Model (I_{gt}).

A.4. VLM-assisted Captioning with Gemini-2.0-Flash

To enable text-driven editing and fine-grained evaluation, we employed **Google Gemini-2.0-Flash** (Team, 2025) for dense captioning. This model was selected for its superior speed and robust multimodal understanding, which are critical for processing large-scale datasets efficiently.

To ensure high-fidelity descriptions, we implemented a category-aware prompting strategy. We designed two distinct sets of structured prompts—one tailored for upper-body garments and another for lower-body garments. This specialization forces the model to attend to the most relevant attributes for each category (e.g., sleeve length and neckline for tops versus cut and pattern placement for bottoms) while strictly enforcing definitive language regarding fabric materials. The specific prompts used for each category are detailed below.

System Prompt: You are a professional fashion analyst. Your task is to describe the top garment worn by the person in the image in a single, descriptive sentence.

User Prompt: Analyze the provided garment image. Your description must definitively state the fabric material, avoiding any words of uncertainty like 'looks like' or 'might be'. Also include the color, sleeve length, and other key details.

Follow the structure of these examples:

Example 1: 'A woman is wearing a red cotton-linen short-sleeved shirt.'

Example 2: 'A man is wearing a black silk long-sleeved shirt.'

Example 3: 'A man is wearing a green nylon vest with zippered pockets.'

Example 4: 'A woman is wearing a sleeveless pure cotton tank top.'

System Prompt: You are a professional fashion analyst. Your task is to describe the pants or skirt worn by the person in the image in a single, descriptive sentence.

User Prompt: Analyze the provided garment image. Your description must definitively state the fabric material, avoiding any words of uncertainty like 'looks like' or 'might be'. Also include the color and other specific details like patterns, text, or features.

Follow the structure of these examples:

Example 1: 'A woman is wearing a red linen skirt with a pattern on the left side and a heart on the right.'

Example 2: 'A man is wearing blue denim jeans with the letters 'ABC' printed on the left leg.'

Example 3: 'A man is wearing black leather pants featuring zippers above the knees.'

Example 4: 'A woman is wearing white silk trousers with a wide-leg cut.'"

B. Additional Details on Evaluation Metrics

B.1. VLM Evaluation Protocol (VLM-as-a-Judge)

Traditional metrics (e.g., FID, SSIM) often fail to capture semantic nuances such as local texture preservation or the preservation of non-edited regions. To address this, we propose a robust VLM-based evaluation protocol utilizing Qwen-VL-Plus as an expert judge. Unlike standard reference-free evaluations, our protocol performs a strict "Reference-based Virtual Try-On" assessment by comparing the generated result against both the source garment image and the ground truth reference image.

The evaluation covers five specific dimensions to ensure a holistic assessment:

1. *Background Consistency:* Ensures non-edited areas remain pixel-perfectly unchanged.
2. *Person Identity & Body Consistency:* Verifies that the model's identity, skin tone, and body structure remain intact.
3. *Texture Fidelity:* Checks for the accurate rendering of fine details (logos, fabrics) from the garment image.

4. *Shape Preservation*: Assesses the geometric correctness of the garment (e.g., sleeve length, neckline, fit).
5. *Overall Realism*: Evaluates lighting, shadows, and the naturalness of folds.

Evaluation Prompt. We designed a structured prompt that forces the VLM to act as a critical fashion image quality evaluator, providing both reasoning and numerical scores for each dimension.

System Prompt for VLM Evaluation

System Prompt: Please evaluate the [Generated Image] based on the following 5 dimensions. Be critical and look for subtle artifacts.

Input Data:

1. **[Garment Image]:** The target clothing (flat lay or mannequin).
2. **[Ground Truth Image]:** The real photo of the person wearing the clothes (Reference for identity, pose, and background).
3. **[Generated Image]:** The AI-generated try-on result.

Task: Compare the [Generated Image] against the references and score it on 5 specific dimensions. Use a scale of 1 to 5 (where 5 is perfect/identical, and 1 is failure).

User Prompt: Please evaluate the [Generated Image] based on the following 5 dimensions. Be critical and look for subtle artifacts.

Dimension 1: Background Consistency

Definition: The background (walls, floor, objects, shadows) must remain pixel-perfectly unchanged compared to the [Ground Truth Image], except for the area occluded by the clothing.

Look for: Distortions, warping near the body, color shifts, or blurring in the non-editing areas.

Scoring:

- 5: Background is identical to Ground Truth.
- 4: Minor color/brightness variations, but no structural changes.
- 3: Noticeable but acceptable blurring or slight warping in small areas.
- 2: Obvious artifacts, warping, or color shifts in multiple areas.
- 1: Obvious warping, noise, or structure changes in the background.

Dimension 2: Person Identity & Body Consistency

Definition: The model's identity (face), skin tone, and body structure (limbs, hands) must match the [Ground Truth Image].

Look for:

- Face: Is the ID preserved? (No face swapping/distortion).
- Body: Are hands/fingers complete and natural? Are arms the correct thickness?
- Skin: Is the skin tone consistent at the neck/arm boundaries?

Scoring:

- 5: Identity preserved perfectly; hands/limbs are flawless.
- 4: Minor imperfections in hands or body edges, but identity intact.
- 3: Noticeable issues with limbs or slight face distortion, but recognizable.
- 2: Significant body deformations or partial identity loss.
- 1: Face distorted, identity lost, or missing/mutated limbs.

Dimension 3: Texture Fidelity

Definition: The fine details from the [Garment Image] (logos, prints, fabric material, complex patterns) must be accurately rendered on the Generated Image. Look for: Blurred logos, disappeared patterns, or wrong fabric material (e.g., silk looking like cotton).

Scoring:

- 5: Texture/Patterns are sharp and strictly consistent with the Garment Image.
- 4: Minor blur in complex patterns, but overall recognizable.
- 3: Noticeable blur or simplification, but main patterns preserved.
- 2: Significant pattern loss or wrong fabric material appearance.
- 1: Logo missing, pattern completely wrong or blurry.

Dimension 4: Shape Preservation

Definition: The geometric style of the clothing from the [Garment Image] must be preserved.

Look for:

- Sleeve Length: Long sleeve vs. Short sleeve vs. Sleeveless.
- Neckline: V-neck vs. Round neck vs. Collar.
- Fit: Baggy vs. Tight.

Scoring:

- 5: The cut and shape perfectly match the specific style of the Garment Image.
- 4: Very minor deviations in fit or cut, but style is correct.
- 3: Noticeable but acceptable deviations (e.g., slightly wrong fit).
- 2: Significant style deviation (e.g., collar shape wrong).
- 1: Wrong category (e.g., long sleeve became short sleeve).

Dimension 5: Overall Realism

Definition: Does the [Generated Image] look like a real photograph? Focus on the fusion of the cloth with the person.

Look for:

- Lighting/Shadows: Do shadows on the cloth match the environment?
- Folds: Are the clothing folds natural (gravity-compliant)?
- Artifacts: Any sticker-like edges, white borders, or blurry patches?

Scoring:

- 5: Indistinguishable from a real photo.
- 4: Very realistic, only minor artifacts under close inspection.
- 3: Acceptable realism, some visible artifacts but believable.
- 2: Obvious artifacts, unnatural folds, or lighting mismatches.
- 1: Fake, obvious collage, or severe artifacts.

Response Format:

You MUST return a complete JSON with BOTH reasoning and scores. **Keep each reasoning analysis concise (max 100 words).**

Example format (you MUST follow this EXACTLY):

```

{
  "reasoning": {
    "background_analysis": "Brief analysis...",
    "person_analysis": "Brief analysis...",
    "garment_analysis": "Brief analysis...",
    "realism_analysis": "Brief analysis..."
  },
  "scores": {
    "background_consistency": 4.5,
    "person_consistency": 4.0,
    "texture_fidelity": 3.5,
    "shape_preservation": 4.0,
    "overall_realism": 4.0
  },
  "final_weighted_score": 4.0
}

```

CRITICAL - You MUST include:

1. "reasoning" object with 4 analysis fields (each max 100 words)
2. "scores" object with all 5 numeric scores (1.0-5.0)
3. "final_weighted_score" (1.0-5.0)
4. NO extra text outside the JSON
5. NO missing fields

B.2. Representation-based Metrics

We compute the Cosine Similarity between the [CLS] tokens of the Reference Garment and the Generated Image using **DINOv3** (Siméoni et al., 2025). To isolate the garment region, we apply the generated segmentation mask to the try-on result before feature extraction.

C. Experimental Details**C.1. Hardware and Software Environment**

All experiments were conducted on a high-performance computing cluster to ensure consistent benchmarking.

- **GPU:** NVIDIA A800 (80GB VRAM) × 8.
- **Frameworks:** PyTorch 2.9.1, CUDA 12.4.
- **Precision:** Mixed precision (BF16 or Float32) was utilized during inference to align with standard deployment environments.

C.2. Baseline Configurations

We evaluate our benchmark against a comprehensive suite of state-of-the-art methods, ranging from diffusion-based virtual try-on pipelines to the latest flow-matching generative models. Unless otherwise specified, all models utilize their official pre-trained checkpoints and recommended inference parameters.

Virtual Try-On & Control-based Methods:

- **OOTD:** We utilized the OOTDsetting, configured with 20 sampling steps and a guidance scale of 2.0 to ensure optimal detail preservation.
- **EasyControl:** Evaluated using the official controllable generation pipeline, ensuring alignment between the conditional input and the generated outfit.

- **UNO**: Deployed using the standard Unified-Model settings for consistent multi-task performance.

Advanced Generative Backbones (Flux Family):

- **FLUX.1-Kontext-dev**: Evaluated using the standard dev-channel configuration.
- **Flux.2-dev**: Evaluated using the latest development checkpoints to assess the capabilities of next-generation flow-matching models.

Commercial & Application-Specific Solutions:

- **NanobananaPro, Qwen-Editor**: Experiments were conducted using their respective official release versions or APIs.
- **HuiWa, YingHui**: For these industry-oriented solutions, we adhered strictly to the provider’s recommended settings to simulate real-world application performance.

D. Additional Experimental Results

D.1. Details of Representation-based Metrics

In the main text (Sec. 3.2.2), we introduced the Multi-scale Garment Fidelity metric (S_{rep}) to evaluate texture quality across different spatial regions. Here, we provide specific implementation details used in our evaluation. **Implementation Parameters.** Referring to Eq. 6 in the main paper, we utilized a standard square structural element B of size 3×3 for morphological operations. We computed the fidelity scores at four distinct scales:

- $k = 0$ ($S_{rep}^{(0)}$): Represents the full garment mask, capturing both boundary alignment and global texture.
- $k = 1, 2, 3$ ($S_{rep}^{(1)}$ to $S_{rep}^{(3)}$): Represent progressively eroded masks. Higher k values exclude the boundary regions, focusing purely on the internal fabric details and reducing the penalty from minor misalignment.

The final reported \bar{S}_{rep} is the arithmetic mean of scores across these scales. The global score S_{global} refers to the standard cosine similarity without mask erosion constraints.

D.2. Correlation Analysis of Metrics

To validate the effectiveness of our proposed VLM and Representation-based metrics, we calculated the correlation coefficients (Spearman ρ_s , Kendall ρ_k , Pearson ρ_p) between these automated metrics and human preference scores. Human judgments were collected from 76 users evaluating 92,072 samples.

Table 6 demonstrates that our VLM-based metrics align closely with human perception, particularly in *Realism* ($\rho_p = 0.990$) and *Identity* ($\rho_p = 0.840$). Table 7 validates the Representation metrics, showing that the averaged multi-scale score (*Avg*) achieves the highest rank correlation ($\rho_s = 0.933$), confirming its robustness in evaluating garment fidelity.

Table 6. VLM Metrics per Dimension. Correlation with Human judgments.

Metric	$\rho_s \uparrow$	$\rho_k \uparrow$	$\rho_p \uparrow$
s_{bg}	0.767	0.556	0.594
s_{id}	0.800	0.667	<u>0.840</u>
s_{tex}	0.767	0.500	0.822
s_{shape}	<u>0.867</u>	<u>0.722</u>	0.806
s_{real}	0.900	0.833	0.990
s_{avg}	0.850	<u>0.722</u>	0.828

Table 7. **Representation Metrics different Dimension.** Correlation with Human judgments. S_{rep_k} corresponds to the erosion level k .

Metric	$\rho_s \uparrow$	$\rho_k \uparrow$	$\rho_p \uparrow$
S_{global}	<u>0.867</u>	<u>0.722</u>	0.687
$S_{rep}^{(0)}$	0.850	0.667	0.741
$S_{rep}^{(1)}$	0.850	0.667	0.709
$S_{rep}^{(2)}$	0.850	0.667	0.695
$S_{rep}^{(3)}$	0.850	0.667	0.708
\bar{S}_{rep}	0.850	0.667	<u>0.712</u>
\bar{S}	0.933	0.833	0.701

D.3. Dataset Visualization

To demonstrate the semantic diversity of OpenVTON-Bench, we visualize representative samples selected from the **20 semantic clusters** identified during our data balancing process using DINOv3 features. As shown in Figure 7, our clustering strategy successfully captures fine-grained distinctions in fashion items, going beyond simple category labels to distinguish material and structural details. The 20 clusters cover a wide spectrum:

- **Distinctive Tops:** The method effectively distinguishes between texture variants, such as *Cropped Knit Tops* (2) versus *V-neck Knit Tops* (3), and isolates specific details like *V-neck Tops with Lace/Embroidery* (13). It also separates basic cuts like *Crew Neck T-shirts* (8) from complex closures like *Button-Front Tops* (9) and *Button-Down Shirts* (10).
- **Outerwear & Sleeves:** The dataset covers varying sleeve lengths and weights, including *Cropped Long-Sleeve Tops* (12), *Hooded Sweatshirts* (6), *Hooded Zip-Up Garments* (19), *Button-Front Coats* (11), and heavy-duty items like *Puffer Vests/Jackets* (16).
- **Bottoms:** We observe a rich variety in lower-body garments, ranging from *Wide-Leg Pants* (0) and *Lace-Up High-Waisted Pants* (1) to *Pleated Skirts* (7), *Shorts with Pockets* (5), *Cargo Shorts* (14), and *Capri Leggings* (15).
- **Dresses:** The clusters differentiate dress silhouettes, including *Sleeveless Bodycon Dresses* (4), *Wrap Dresses with Ruching* (17), and *A-line Dresses* (18).

This granular separation (e.g., distinguishing simple knits from lace-detailed tops) confirms that our sampling strategy preserves high-frequency visual details essential for robust VTON evaluation.

D.4. Extended Qualitative Comparison

We provide a comprehensive visual comparison of all benchmarked methods. Figure 8 illustrates the generation results for **every baseline model** evaluated in the main paper.

For each model, we present **10 generated samples** corresponding to challenging input scenarios from our benchmark. This allows for a holistic assessment of each model’s ability to handle intricate details (e.g., text, logos) and maintain garment integrity under complex poses.

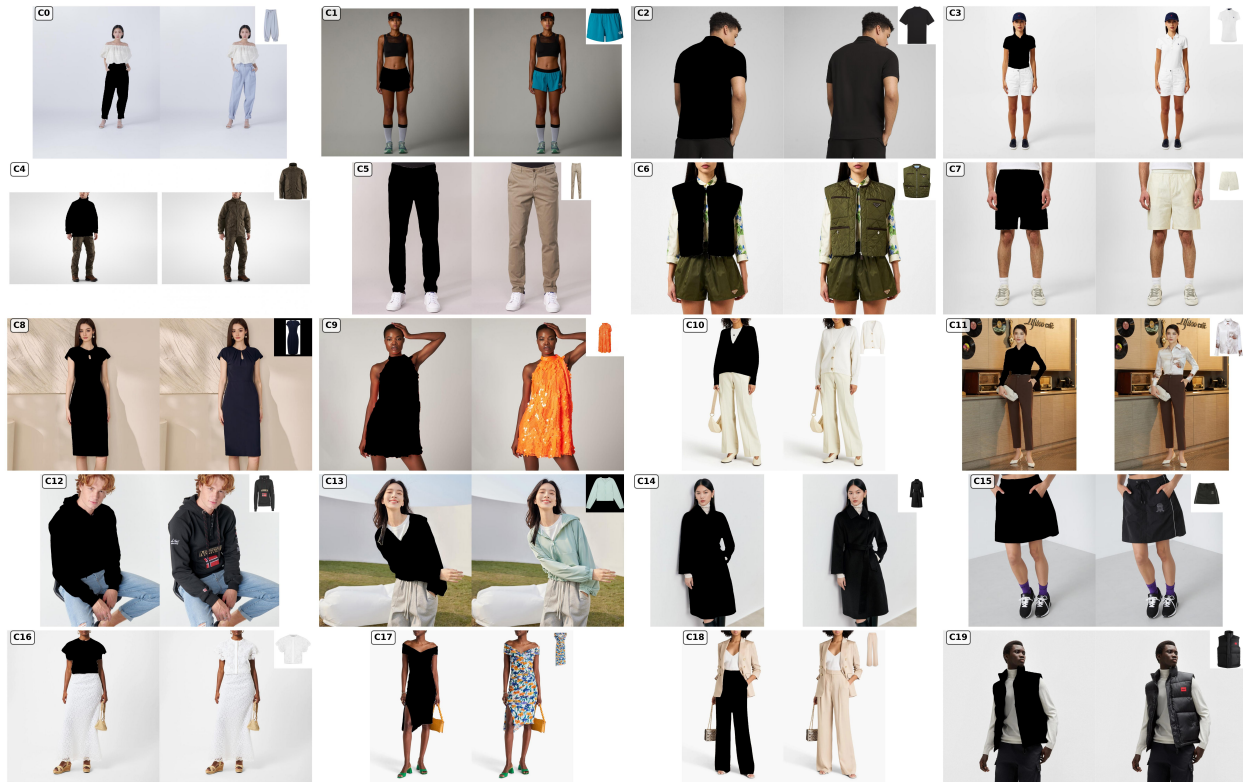


Figure 7. Diversity of OpenVTON-Bench. We display representative triplets (Garment, Model, Mask) sampled from the 20 distinct semantic clusters defined in Appendix D.3.



Figure 8. Qualitative comparison of different models.